

Activity, diffusion, and correlations in a two-dimensional conserved stochastic sandpile

Sharon Dantas da Cunha¹, Luciano Rodrigues da Silva^{2,3},
Gandhimohan M. Viswanathan² and Ronald Dickman^{4,5}

¹Escola de Ciências e Tecnologia, Universidade Federal do Rio Grande do Norte, Campus Universitário, 59078-970 Natal, Rio Grande do Norte, Brazil

²Departamento de Física Teórica e Experimental, Universidade Federal do Rio Grande do Norte, Campus Universitário, 59078-900 Natal, Rio Grande do Norte, Brazil

³National Institute of Science and Technology of Complex Systems, Universidade Federal do Rio Grande do Norte, Campus Universitário, 59078-900 Natal, Rio Grande do Norte, Brazil

⁴Departamento de Física, ICEX, Universidade Federal de Minas Gerais, Caixa Postal 702, 30161-970 Belo Horizonte, Minas Gerais, Brazil

⁵National Institute of Science and Technology of Complex Systems, Caixa Postal 702, 30161-970 Belo Horizonte, Minas Gerais, Brazil

E-mail: sharondantas@ect.ufrn.br, luciano@dfte.ufrn.br, gandhi@dfte.ufrn.br and dickman@fisica.ufmg.br

Abstract.

We perform large-scale simulations of a two-dimensional restricted-height conserved stochastic sandpile, focusing on particle diffusion and mobility, and spatial correlations. Quasistationary (QS) simulations yield the critical particle density to high precision [$p_c = 0.7112687(2)$], and show that the diffusion constant scales in the same manner as the activity density, as found previously in the one-dimensional case. Short-time scaling is characterized by subdiffusive behavior (mean-square displacement $\sim t^\gamma$ with $\gamma < 1$), which is easily understood as a consequence of the initial decay of activity, $\rho(t) \sim t^{-\delta}$, with $\gamma = 1 - \delta$. We verify that at criticality, the activity correlation function $C(r) \sim r^{-\beta/\nu_\perp}$, as expected at an absorbing-state phase transition. Our results for critical exponents are consistent with, and somewhat more precise than, predictions derived from the Langevin equation for stochastic sandpiles in two dimensions.

PACS numbers: 05.70.Ln, 05.50.+q, 05.65.+b

1. Introduction

Sandpile models are the best known examples of self-organized criticality (SOC) [1, 2, 3, 4, 5], in which the dynamics of a system forces it to the critical point of an absorbing-state phase transition [6, 7] leading to scale-invariance in the apparent absence of tunable parameters [8]. The SOC state can be attributed to the presence of two well separated time scales [8, 9, 10, 11], one corresponding to the external energy input or driving force, and the other to the microscopic evolution (e.g., avalanches). The separation between the two times scales (also called *slow driving*) effectively tunes the system to the neighborhood of an absorbing-state phase transition; the latter transition is reached in the usual manner, by adjusting a control parameter, in models known as *conserved sandpiles* (CS) or *fixed-energy sandpiles* [6, 12, 13, 14, 15]. The CS has the same local dynamics as the corresponding driven sandpile, but a fixed number of particles. It is characterized by a nonconserved order parameter (the activity density) which is coupled to a conserved field [16] whose evolution is arrested in space-time regions devoid of activity.

In recent years, a number of studies have characterized the critical properties of conserved stochastic sandpiles (CSS). As is usual in studies of critical phenomena, theoretical discussions of scaling and universality are anchored in the analysis of a continuum field theory or of a Langevin equation (i.e., a nonlinear stochastic partial differential equation) that reproduces the phase diagram and captures the fundamental symmetries and conservation laws of the system. In the case of CSS, these symmetries and conservation laws define the *conserved directed percolation* (CDP) universality class [16]. Extensive numerical studies of a Langevin equation corresponding to CDP are described in [17, 18]. The critical exponent values reported in [17] are in good agreement with simulations of conserved lattice gas models [19, 20], which exhibit the same symmetries and conservation laws as CSS. There is now strong evidence that the CSS belongs to the CDP universality class [21, 22], although the existence of this class has been questioned by Basu *et al.* [23]. According to these authors, the CSS belongs to the usual directed percolation (DP) class; further studies are required to verify this assertion.

Most studies of CSS characterize the critical region using the order parameter (the activity density ρ , i.e., the fraction of active sites) [9, 21, 24]. In this work we study the diffusion particles in a two-dimensional CSS to characterize the phase transition through the diffusion constant D , defined via the mean-square particle displacement. Dhar and Pradhan suggested D and the order parameter would be proportional in Abelian sandpiles [25, 26]. An earlier study by some of the present authors verified that D scales in the same manner as the activity density in the stationary regime in one-dimensional stochastic sandpiles [27]. Dimensionality appears to play a nontrivial role in defining the universality of CSS [23, 28], in particular, different relations between CSS and DP, and between CSS and an elastic interface model, in one and two dimensions. Thus it is of interest to verify the relation between D and ρ in the two-dimensional case

as well. In addition, we study (for the first time, to our knowledge), the static activity correlation function and the particle mobility in the CSS.

The remainder of this paper is organized as follows. In Sec. 2 we define the models. In Sec. 3 we report simulation results for the diffusion constant and the order parameter, and perform scaling analyses to extract estimates for the critical exponents. We close in Sec. 4 with a summary of our results.

2. Model

We study modified conserved stochastic sandpiles, related to Manna’s model [29, 30], called the *restricted-height sandpile* in the standard version studied in [21, 24, 27]. In addition we study the effect of a weak force or “drive” f directed along one of the lattice directions to determine the particle mobility. The model is defined on square lattice of $L \times L$ sites, with periodic boundaries; the configuration is specified by the number of particles, $z_{i,j} = 0, 1, \text{ or } 2$, at each site (i, j) . Sites with $z_{i,j} = 2$ are *active*, while those with $z_{i,j} \leq 1$, are said to be *inactive*. No site may harbor more than two particles.

The temporal evolution consists of a series of *toppling* events, in which two particles are transferred from an active site to one or more of its first neighbors $[(i - 1, j), (i + 1, j), (i, j - 1), (i, j + 1)]$ with equal probabilities. The target sites for the two particles are chosen independently. If a particle attempts to jump to a site already bearing two particles, it returns to the toppling site. The evolution follows a continuous-time Markovian dynamics in which each active site has a transition rate of unity to topple. At each step of the evolution, one of the current N_a active sites is chosen at random to topple; the time increment associated each step is $\Delta t = 1/N_a$. In this way, each active site waits, on average, one time unit before toppling.

In conserved sandpiles, the particle density, $p = N/L^d$, serves as a temperature-like control parameter [6]. Below the critical value, p_c , the system eventually reaches an absorbing configuration ($N_a = 0$). For $p > p_c$, by contrast, the activity continues indefinitely ($N_a > 0$), in the infinite-size limit. The order parameter associated with the phase transition is the activity density, given by the fraction of active sites, $\rho = N_a/L^2$. Although activity *must* continue indefinitely if $p > 1$, remarkably, p_c is in fact well below unity. For the model studied here, the best estimate for the critical density is $p_c = 0.7112687(2)$, as shown below.

3. Simulation method and results

In this section we discuss our results, first for the usual restricted-height sandpile, and then for the model under a weak drive. In both cases, we study system sizes $L = 32$ to 2048. Random numbers are generated using the GNU Scientific Library for C++ [31]. Initial configurations are generated by inserting N particles randomly on a square lattice of $L \times L$ sites, subject to the restriction $z_{i,j} \leq 2$.

3.1. Locating the critical point

We performed three sets of studies: two in the immediate vicinity of critical point p_c , and a third in the supercritical region. Initially, we determine the value of p_c using the moment ratio $m = \langle \rho^2 \rangle / \rho^2$ in quasistationary (QS) simulations [32]. This method samples the QS probability distribution, i.e., the probability distribution at long times, conditioned on survival; for details on the method see [32]. The number of realizations used to obtain m varies from 48 (smallest size) to 16 (largest size). Since the particle density can only be varied in steps of $1/L^2$, estimates for properties at intermediate values of p are obtained via interpolation. Figure 1 shows $m(p)$ in the immediate vicinity of p_c for $L = 256 - 2048$. The critical point p_c is characterized by a finite limiting value, m_c [33], so that p values for which m appears to grow or decrease without limit (corresponding to the sub- and supercritical regimes, respectively), can be excluded as being off-critical. On the basis of these data, we estimate $p_c = 0.7112687(2)$.

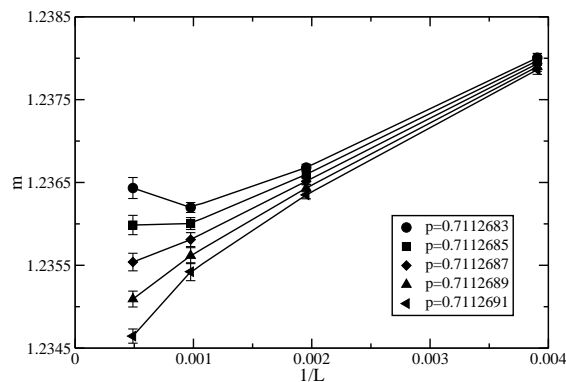


Figure 1. Moment ratio m versus system size for particle densities in the immediate vicinity of p_c .

3.2. The subdiffusive regime

Next we turn to an analysis of the diffusion coefficient D , defined via the usual relation:

$$\langle [\Delta x]^2 + [\Delta y]^2 \rangle = 4Dt \quad (1)$$

For each particle k , let $\Delta x_k(t) = h_{x,k}^+(t) + h_{x,k}^-(t)$ and $\Delta y_k(t) = h_{y,k}^+(t) + h_{y,k}^-(t)$ represent its displacement since time zero in the x and y directions, respectively, due to toppling events. The counting variables $h_{i,k}^\pm(t)$ denote the number of hops taken by particle k along direction i , in the positive and negative directions, respectively, up to time t . The angular brackets in Eq. (1) denote an average over particles and over independent realizations of the process. Note that D as defined above is, in general, a function of time, though we expect it to attain a stationary value at long times.

Since the displacements of a given particle at successive toppling events are independent, we expect the msd to grow linearly with the number of topplings. Although

not all displacement attempts are successful (the height restriction causes some to be rejected), in the stationary regime the fraction of successful attempts η_s is time-independent, as is the density ρ of active sites. (By $\eta_s(t)$ we mean the number of particles that change their position during the interval $[t, t + \Delta t]$ divided by twice the number of toppling events during this interval.) Thus the msd should grow linearly with *time* in the stationary regime, as is verified here and in the one-dimensional case [27]. By the same reasoning, if η_s and/or ρ vary with time, we should expect deviations from the linear relation $\langle [\Delta x]^2 + [\Delta y]^2 \rangle \propto t$.

For p near p_c , the initial activity density generated by random particle insertion is much larger than the stationary activity density. This is easily seen by noting that, during the insertion process, setting the rate of particle insertion *attempts* at one particle per site and per unit time, s the fractions $f_j(s)$ of sites bearing exactly j particles satisfy the equations ‡:

$$\frac{df_0}{ds} = -f_0, \quad \frac{df_1}{ds} = f_0 - f_1, \quad \text{and} \quad \frac{df_2}{ds} = f_1. \quad (2)$$

Since the lattice is empty at time zero we have, $f_0 = e^{-s}$, $f_1 = se^{-s}$, and $f_2 = 1 - (1 + s)e^{-s}$. The process stops when the particle density $f_1 + 2f_2$ reaches the desired value p . (Thus the stopping time s_f is related to p via a transcendental equation.) For particle density $p_c \simeq 0.71127$, this yields an initial activity density of $f_2 \simeq 0.1778$, much larger than the stationary activity density, which in fact tends to zero as $L \rightarrow \infty$ at $p = p_c$. Thus we should expect the activity density $\rho(t)$ to decrease initially.

In fact, we can divide the sandpile evolution into four regimes, as shown in Fig. 2 (a): (1) an initial transient; (2) the subdiffusive regime, in which the msd grows more slowly than linearly while ρ decays as a power law; (3) a regime of anomalous growth in the activity $\rho(t)$; (4) the stationary regime. Analogous time evolution of the activity is reported in simulations of a Langevin equation for the two-dimensional CSS in Ref. [17]. In the the subdiffusive we find $\langle [\Delta x]^2 + [\Delta y]^2 \rangle \propto t^\gamma$, with $\gamma < 1$, as determined via a least-squares linear fit to the msd data on log scales. Figure 2 (b) shows that the fraction η_s of successful particle displacement attempts increases slowly with time in the subdiffusive regime, but not enough to compensate for the sharp reduction in ρ . The steady decrease in $\rho(t)$ therefore generates sublinear growth in the msd.

The msd, $\langle [\Delta x]^2 + [\Delta y]^2 \rangle$ is plotted versus time in Fig. 3 (a) for three values of p in the supercritical regime; the crossover between the short-time subdiffusive regime and the long-time linear regime is evident. Figure 3 (b) shows the dependence of γ on $\Delta \equiv p - p_c$ in the subdiffusive regime. We note that, away from criticality, γ is not expected to represent a universal scaling property. At the critical point, we expect the power-law decay $\rho(t) \sim t^{-\delta}$ in the initial (“short-time”) scaling regime. We verify this scaling law at criticality, in the subdiffusive regime in Fig. 4. Our results

‡ To avoid confusion, we denote the time variable associated with the initial filling process by s . When the particle density has attained its desired value p , $s = s_f$

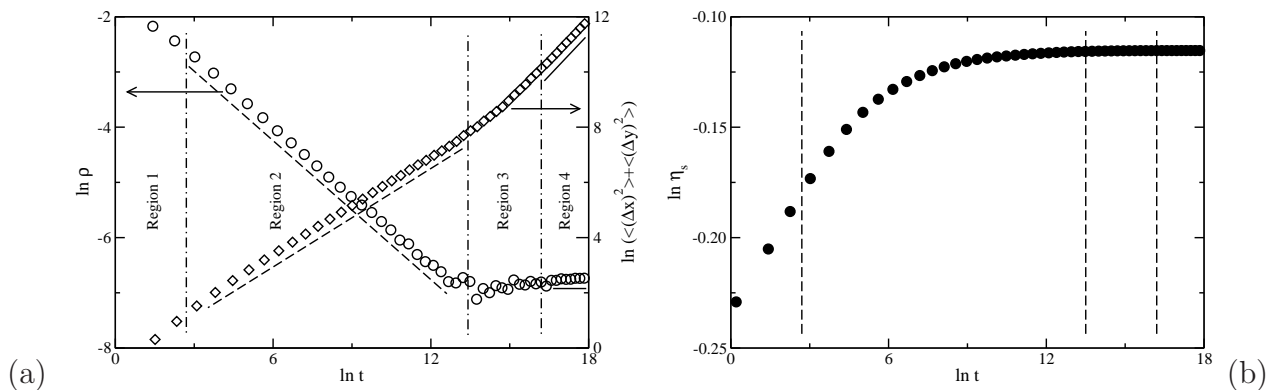


Figure 2. (a) msd and ρ versus time for system size $L = 2048$ and particle density $p = 0.711315$, slight above p_c . The solid lines correspond the stationary regime (region “4”), broken lines to the subdiffusive regime (region “2”). (b) Fraction of successful transfer attempts η_s versus time t .

yield $\delta = 0.436(2)$, $0.439(3)$, and $0.427(2)$ for system sizes $L = 512$, 1024 , and 2048 , respectively; we adopt $\delta = 0.43(1)$ as our best estimate. For system size $L = 2048$ we find $\gamma = 0.585(1)$ at criticality. We expect each particle to execute a random walk in which the number of steps per unit time is proportional to the activity density ρ . Thus, in the subdiffusive regime, particle diffusion can be described qualitatively by a Langevin equation,

$$\frac{d\mathbf{x}}{dt} = \mathbf{A}(t) \quad (3)$$

in which the noise satisfies $\langle A_i(t)A_j(s) \rangle = \Gamma\delta_{ij}\rho(t)\delta(t-s)$ (here Γ is a constant and i and j are Cartesian indices). Integrating the Langevin equation one readily finds that the msd grows $\propto t^{1-\delta}$, implying that $\gamma + \delta = 1$. Our numerical results are essentially consistent with this, yielding $\gamma + \delta = 1.015(11)$.

3.3. Static scaling behavior

Next we analyze the stationary values of ρ , D and τ (the mean lifetime) in the critical region. For the two first parameters, we use QS simulations. The number of realizations varies from 1024 (for $L = 32$) to 16 (for $L = 2048$). To begin, we estimate ρ and D at the critical point; ρ is expected to scale with system size as $\rho \sim L^{-\beta/\nu_\perp}$. Our results permit us to estimate critical exponent ratio, and confirm that D and ρ scale in the same manner, as can be seen in Fig. 5 (a).

The mean lifetime τ is determined from the probability $P(t)$ that the activity survives up time t . We used conventional (not QS) simulations in this case. The number N_s of independent realizations used in this set varies from 65536 (for the smallest size) to 1024 (for the largest). We verify that $P(t)$ decays exponentially, so that the mean lifetime can be defined via $P(t) \sim \exp(-t/\tau)$. At the critical point, standard finite-size

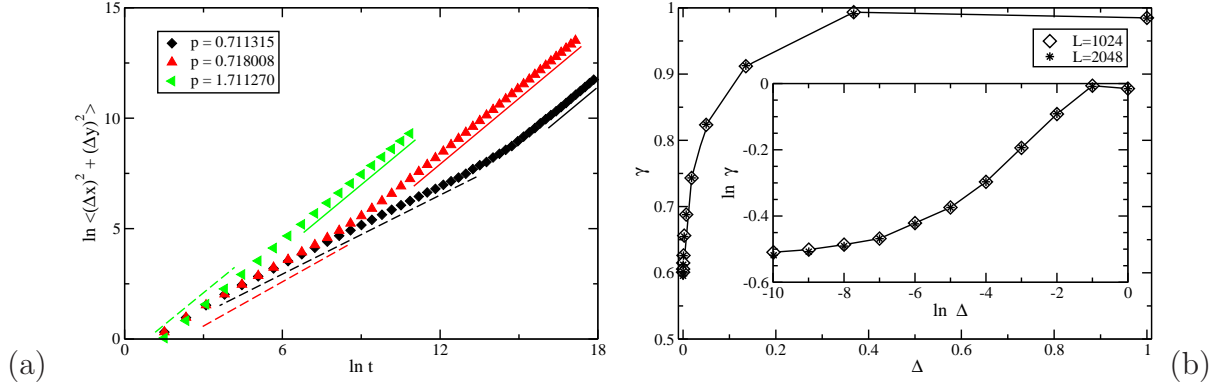


Figure 3. (Color online) (a) msd versus time for $L = 2048$ and p values as indicated. The solid lines have a slope of unity; the slopes of the broken lines γ vary from ≈ 0.60 to ≈ 0.98 . (b) γ versus $\Delta = p - p_c$ in the subdiffusive regime. Inset: the same data on logarithmic scales.

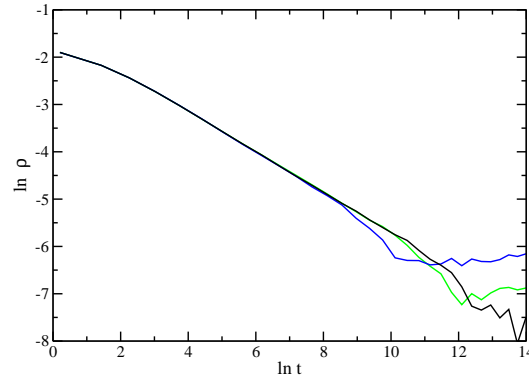


Figure 4. Activity density ρ versus time t at $p = p_c$, for system sizes (upper to lower at right) $L = 512, 1024,$ and 2048 .

scaling arguments yield $\tau \sim L^z$, with z the dynamical exponent, given by the scaling relation $z = \nu_{\parallel}/\nu_{\perp}$. Discarding the initial transient of each study, the survival time τ is estimated by fitting of the exponential tail of $P(t)$, as well as by determining the time required for the survival probability to decay to one half [9]. Since the particle density can only be varied in steps of $1/L^2$, estimates for properties at intermediate values of p are obtained via interpolation. Figure 5 (a) shows the behavior of ρ , D and τ at the critical point. Using least-squares linear fits to the data for ρ , D and τ , we obtain the estimates $\beta/\nu_{\perp} = 0.768(8)$, $\beta/\nu_{\perp} = 0.779(6)$ and $z = 1.519(8)$, respectively.

We determine the correlation length exponent ν_{\perp} in the following manner. In the immediate vicinity of critical point, the derivatives of the moment ratio and of $\ln \rho$ with

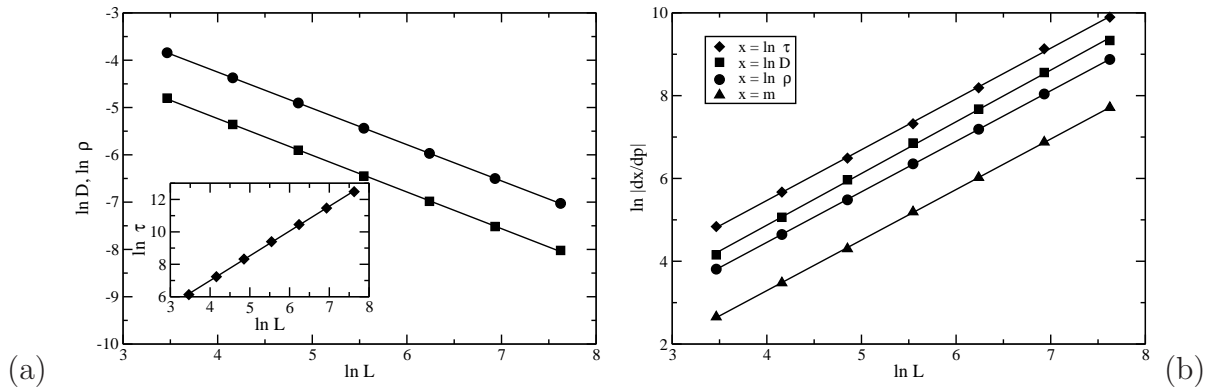


Figure 5. (a) Diffusion constant D (squares) and stationary order parameter ρ (circles) versus system size L at the critical point. The slopes of the straight lines are (lower to upper) 0.768(6) and 0.779(6). Inset: lifetime τ (diamonds) versus L ; the slope of the straight line is 1.519(8). (b) Derivatives of (lower to upper) m , $\ln \rho$, $\ln D$ and $\ln \tau$ with respect to particle density, evaluated at p_c , versus system size L . The slopes of straight lines are $\approx 1.234(8)$.

respect to p scale as [9]:

$$\left| \frac{\partial m}{\partial p} \right|_{p_c} \propto L^{1/\nu_{\perp}} \quad (4)$$

and

$$\left| \frac{\partial \ln \rho}{\partial p} \right|_{p_c} \propto L^{1/\nu_{\perp}} \quad (5)$$

Similar behaviors hold for the derivatives of $\ln D$ and $\ln \tau$. (The derivatives are estimated numerically using the central difference method, using the values of $\ln \rho$, $\ln D$ and $\ln \tau$ above, below and at p_c .) Figure 5 (b) shows the derivatives as a function of system size. Least-squares linear fits to the data yield $\nu_{\perp} = 0.818(6)$, $\nu_{\perp} = 0.817(6)$, $\nu_{\perp} = 0.795(6)$ and $\nu_{\perp} = 0.811(6)$ for m , $\ln \rho$, $\ln D$ and $\ln \tau$, respectively, for a global estimate of $\nu_{\perp} \approx 0.812(7)$. Then, using $\beta/\nu_{\perp} = 0.779(6)$ obtained above, we find $\beta = 0.633(6)$. Similarly, using $z = \nu_{\parallel}/\nu_{\perp} = 1.512(8)$, we find $\nu_{\parallel} = 1.225(7)$.

3.4. Supercritical regime

We determined the stationary activity density and diffusion rate for a series of particle densities p in the supercritical regime, using QS simulations. In this set, the number of realizations varies from 512 (smallest size) to 8 (largest size) for values of p near p_c , and 3 for values distant from p_c . The time required for the diffusion constant to reach its stationary value is somewhat greater than for the order parameter, e.g., $t_D = 3 \times 10^7$ and $t_{\rho} = 2 \times 10^7$ for the largest system studied and $p = 0.7112692$. Figure 6 shows the stationary values of D and ρ versus $\Delta = p - p_c$. Several observations can be made: 1) for the largest systems studied, D and ρ converge to their limiting ($L \rightarrow \infty$) values for

$\Delta \geq 0.0025$ and $\Delta \geq 0.0015$ respectively; 2) even for values of Δ such that the diffusion rate has converged, the slope of $D(\Delta)$ on logarithmic scales changes appreciably with Δ , making a reliable estimate of the critical exponent β difficult, using these data; and 3) D drops sharply when $p \rightarrow 2$, due to the height-restriction, which inhibits the particle motion. These tendencies are also observed in the one-dimensional model, as can be seen in Fig. 7. Since the curvature of $\ln \rho$ and $\ln D$ as functions of $\ln \Delta$ is less pronounced in the two-dimensional case, we performed linear fits to the data for ρ and D on intervals for which the curvature of the log-log plot is minimal (that is, for $-8 \leq \ln \Delta \leq -2$, and $-10 \leq \ln \Delta \leq -3$, respectively). The resulting estimates for the critical exponent β are 0.64(1) (from the activity density data) and 0.62(1) (from the diffusion coefficient); these values are in reasonable agreement with the estimate obtained above via scaling analysis.

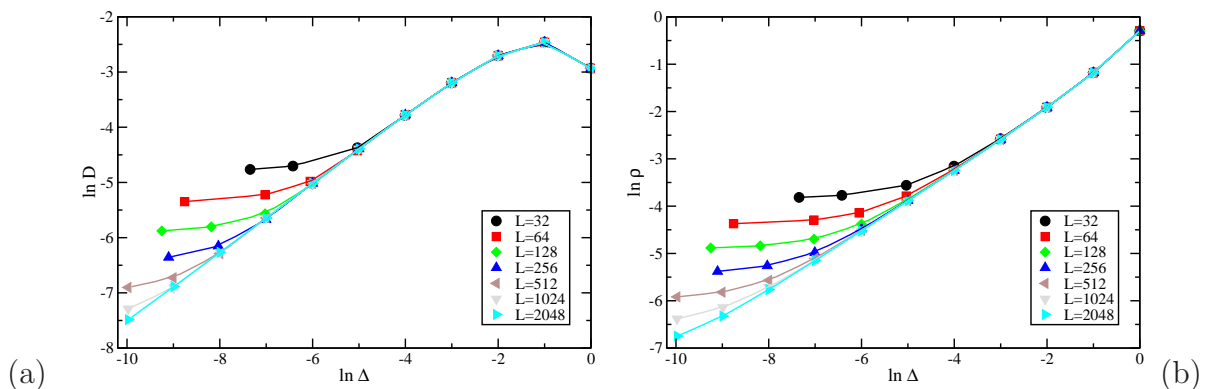


Figure 6. (Color online) (a) Diffusion rate versus Δ for system sizes as indicated. Error bars are smaller than symbols. (b) Stationary activity density ρ versus Δ .

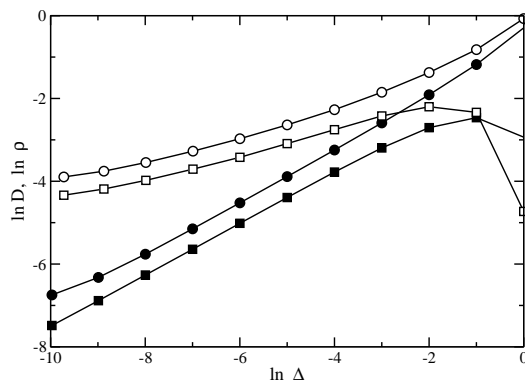


Figure 7. Stationary activity (circles) and asymptotic diffusion rate (squares) versus Δ in one dimension (open symbols), system size $L = 50000$, and two dimensions (filled symbols), system size $L = 2048$.

From Fig. 6, it is clear that neither $D(\Delta)$ nor $\rho(\Delta)$ have a simple power-law dependence on Δ , even for parameter values such that there is no discernible finite-size effect

for D and ρ . In the case of the diffusion constant, the data collapse for $\Delta \geq 0.018$, for all sizes studied, and $\Delta \geq 0.00013$, for $L = 1024$ and $L = 2048$. The activity exhibits a rather similar behavior when $\Delta \rightarrow 0$. In Fig. 8 we test whether the data for the scaled activity, $\rho^* = L^{\beta/\nu_\perp} \rho$, collapse when plotted versus the scaled distance from criticality, $\Delta^* = L^{1/\nu_\perp} \Delta$. Data collapse is observed only quite near the critical point, consistent with previous studies of the CSS [21, 27]. D and ρ collapse with the same critical parameters. The critical exponents obtained via data collapse are $\beta = 0.64(1)$ and $\nu_\perp = 0.84(1)$. These results are consistent with the critical exponents found using our first set of simulations, and with the best numerical estimates obtained from simulations of the Langevin equation: $\beta = 0.66(2)$, $\nu_\perp = 0.84(2)$, and $\nu_\parallel = 1.27(7)$ [17].

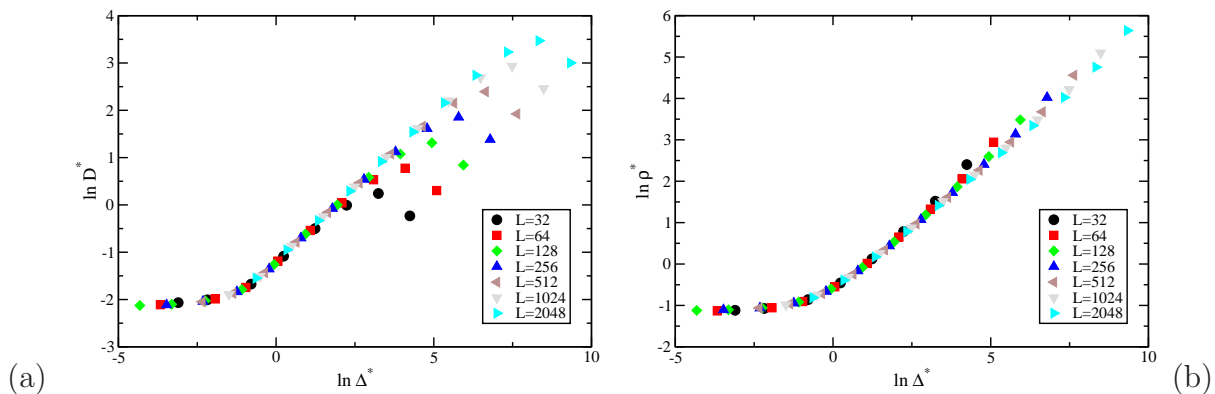


Figure 8. (Color online) (a) Scaled diffusion rate D^* versus scaled distance from critical point Δ^* , as defined in text. (b) Scaled activity ρ^* versus Δ^* .

3.5. Activity correlation function

To our knowledge, few if any studies have been performed on spatial correlations of the activity in stochastic sandpiles. Here we use QS simulations to determine the static correlation function, defined via

$$C(r) = \langle A_{i,j} A_{k,l} \rangle - \langle A_{i,j} \rangle \langle A_{k,l} \rangle \quad (6)$$

where $r = \sqrt{(i-k)^2 + (j-l)^2}$ and $A_{i,j} \equiv 1$ if $z_{i,j} = 2$, and is zero otherwise. (That is, $A_{i,j}$ is the indicator variable for activity at the site.) Note that $\langle A_{i,j} \rangle = \rho$. At the critical point of an absorbing-state phase transition, correlations are expected to decay as a power law, $C(r) \propto r^{-\beta/\nu_\perp}$, for $r \ll L$ [34]. In Fig. 9 (a) we plot $C^*(r) = L^{\beta/\nu_\perp} C(r)$ for $L = 1024$ and $L = 2048$, using the estimate for β/ν_\perp obtained above; evidently the two curves collapse, and follow essentially the same power law. For $r = L/2$ the correlation function attains a minimum, as expected due to the periodic boundaries conditions. To obtain the decay exponent we analyze the local slope ϕ (see Fig. 9 (b)), obtained from a linear fit to the data for $\ln C$ versus $\ln r$ (the points being equally spaced in $\ln r$), fixing the initial point $r_i = 2$ and varying the final point r_f included in

the fitting interval. The resulting values for β/ν_{\perp} yield the estimate 0.777(8), consistent with our previous result.

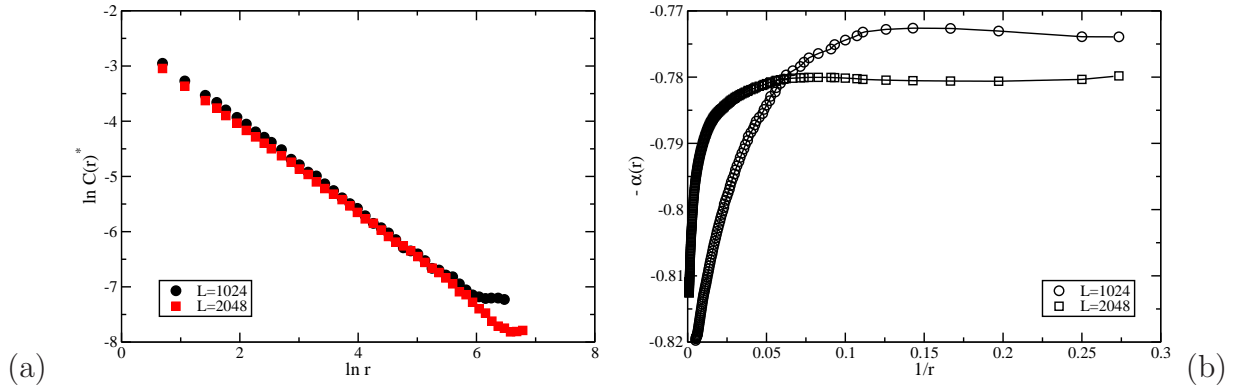


Figure 9. (a) The Static correlation function modified $C^*(r)$ versus r for $L = 1024$ and $L = 2048$. (b) Estimate for the exponent $\alpha = \beta/\nu_{\perp}$ versus $1/r_f$, as defined in text.

3.6. Particle mobility

In a stochastic system in which the particles are subject a weak force or bias f , we expect the mean displacement per unit time to follow $\langle \Delta x \rangle / t = \mu f$, where we have assumed the force acts along the x direction, and μ denotes the mobility. We implement the bias by altering the probabilities $p(i', j')$ to hop from site (i, j) to a neighbor (i', j') as follows: $p(i-1, j) = 1/4 - f$; $p(i+1, j) = 1/4 + f$; $p(i, j-1) = p(i, j+1) = 1/4$, with $f \ll 1$. Figure 10 (a) shows $\langle \Delta x(t) \rangle / t \equiv \bar{v}$ as a function of f for several values of p , and system sizes $L = 1024$ and 2048 , in the stationary regime. Note that \bar{v} is independent of system size, and is proportional to f , as expected.

If particle hopping events were mutually independent, we would expect a simple relation (analogous to the Stokes-Einstein relation of Brownian motion) to hold between μ and D . To see this, note that at each particle displacement, $\langle (\Delta x)^2 + (\Delta y)^2 \rangle = 1$, and that the fraction of particles residing at active sites is $2\rho/p$. Thus, assuming independence, the particle msd (averaged over all particles) during a time interval t is $2\eta_s \rho t / p$, yielding $D = \rho \eta_s / 2p$. Under a bias f , the mean displacement along the x direction per particle displacement is $\langle \Delta x \rangle = 2f$, so that $v = 4\eta_s \rho f / p$, which implies $\mu/D = 8$. In fact, the ratio μ/D remains close to this value over most of the range of particle densities of interest, as shown in the inset of Fig. 10. Finally, the simplistic prediction $pD/(\rho \eta_s) = 1/2$ is tested in Fig. 11. We see that the ratio remains close to, but smaller than, the predicted value, over most of the range of interest, with more significant deviations neat the critical point and for p approaching 2. The discrepancies between the simplistic predictions for μ/D and $pD/(\rho \eta_s)$ and the values observed in simulations presumably reflect correlations between occupancies of nearby sites.

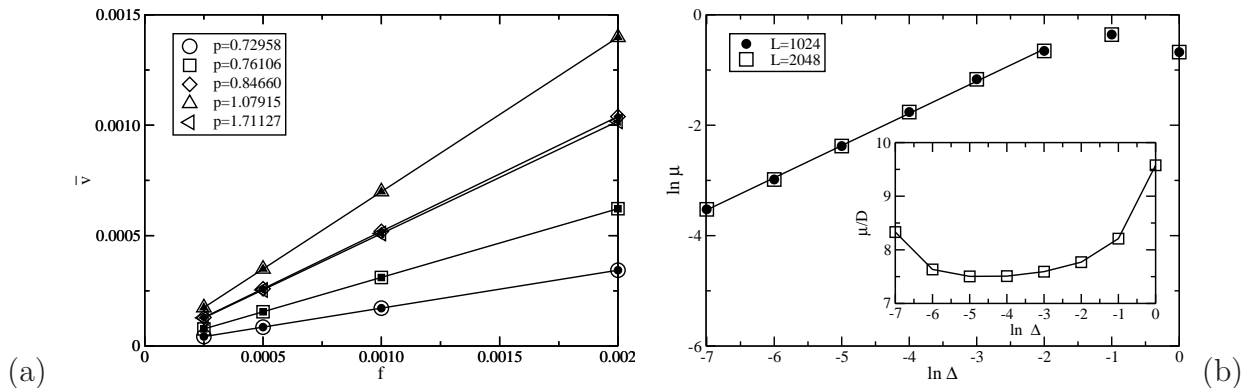


Figure 10. (a) Mean rate of particle displacement \bar{v} versus bias f for particle densities p as indicated and system sizes $L = 1024$ (filled symbols) and 2048 (open symbols). (b) μ versus Δ . The slope of the solid line is 0.5829(1). Inset: Stationary value of μ/D versus Δ for system size $L = 2048$ (values for other sizes are identical). Lines are a guide for the eye; error bars are smaller than symbols.

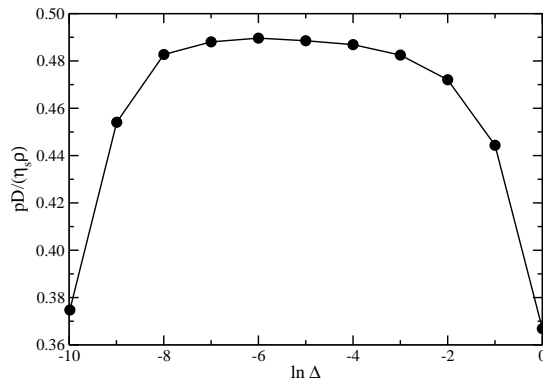


Figure 11. Stationary ratio $pD/(\eta_s \rho)$ versus Δ for system size $L=2048$.

4. Conclusions

In summary, we study diffusion in a restricted-height conserved stochastic sandpile in two dimensions, determining the critical particle density p_c to high precision. Our results show that, as expected, the diffusion constant scales in the same manner as the order parameter. An analogous result was shown previously for several one-dimensional conserved stochastic sandpiles [27]. At short times we observe subdiffusive behavior, i.e., a msd growing $\sim t^\gamma$ with $\gamma < 1$. This reflects the steady initial decay of activity (which follows a power law at criticality, $\rho \sim t^{-\delta}$) and does not imply anomalous diffusion, since the msd in fact grows linearly with the number of topplings, so that $\gamma = 1 - \delta$ at criticality.

	Langevin	present work
β/ν_{\perp}	0.85(8)	0.77(1)
ν_{\perp}	0.84(2)	0.82(1)
z	1.51(3)	1.512(8)
β	0.66(2)	0.63(1)
δ	0.50(5)	0.43(1)

Table 1. Summary of results for critical exponents characterizing the two-dimensional conserved stochastic sandpile. Results in the column labeled “Langevin” are from Ref. [17].

Our estimates for critical exponents, summarized in Table I, are consistent with studies based on the Langevin equation [17]. The somewhat higher precision of the present study derives in good part from the precision of our estimate for the critical density, $p_c = 0.7112687(2)$. The associated critical moment ratio is $m = 1.2354(2)$. The activity density and diffusion constant exhibit a finite-size scaling collapse of data over a restricted range of particle densities, although somewhat larger than in the one-dimensional CSS. Overall, our results support a fairly simple scaling picture for the two-dimensional CSS, including the stationary correlation function for the activity. This is in contrast to the one-dimensional case, which is marked by anomalous scaling behavior, and for which the issue of asymptotic DP-like scaling remains open.

Acknowledgements

This work is supported by CNPq, Brazil.

References

- [1] Bak P, Tang C and Wiesenfeld K, 1987 *Phys. Rev. Lett.* **59** 381
- [2] Bak P, Tang C and Wiesenfeld K, 1988 *Phys. Rev. A* **38**, 364
- [3] Jensen H J, 1998 *Self-Organized Criticality, Emergent Complex Behavior in Physical and Biological Systems* (Cambridge: Cambridge University Press)
- [4] Pruessner G, 2012 *Self-Organised Criticality* (Cambridge: Cambridge University Press)
- [5] Dhar D, 1999 *Physica A* **263** 4
- [6] Dickman R, Muñoz M A, Vespignani A and Zapperi S, 2000 *Braz. J. Phys.* **30** 27
- [7] Muñoz M A, Dickman R, Pastor-Satorras R, Vespignani A and Zapperi S, 2001 Sandpiles and absorbing-state phase transitions: Recent results and open problems *Modeling Complex Systems: Sixth Granada Lectures on Computational Physics (AIP Conference Proceedings vol 574)* ed J Marro and P L Garrido (New York: American Institute of Physics)
- [8] Grinstein G, 1995 Generic scale invariance and self-organized criticality *Scale Invariance, Interfaces and Nonequilibrium Dynamics (NATO Advanced Study Institute, Series B: Physics vol 344)* ed A. McKane *et al.* (New York: Plenum Press)
- [9] Vespignani A, Dickman R, Muñoz M A and Zapperi S, 2000 *Phys. Rev. E* **62** 4564
- [10] Vespignani A and Zapperi S, 1997 *Phys. Rev. Lett.* **78** 4793
- [11] Vespignani A and Zapperi S 1998 *Phys. Rev. E* **57** 6345

- [12] Tang C and Bak P, 1988 *Phys. Rev. Lett.* **60** 2347
- [13] Paczuski M, Maslov S and Bak P, 1996 *Phys. Rev. E* **53** 414
- [14] Dickman R, Vespignani A and Zapperi S, 1998 *Phys. Rev. E* **57** 5095
- [15] Vespignani A, Dickman R, Muñoz M A and Zapperi S, 1998 *Phys. Rev. Lett.* **81** 5676
- [16] Rossi M, Pastor-Satorras R and Vespignani A, 2000 *Phys. Rev. Lett.* **85** 1803
- [17] Ramasco J J, Muñoz M A and da Silva Santos C A, 2004 *Phys. Rev. E* **69** 045105(R)
- [18] Dornic I, Chaté H and Muñoz M A, 2005 *Phys. Rev. Lett.* **94** 100601
- [19] Pastor-Satorras R and Vespignani A, 2000 *Phys. Rev. E* **62** R5875
- [20] Kockelkoren J and Chaté H, 2003 *arXiv:cond-mat/0306039*
- [21] Dickman R, 2006 *Phys. Rev. E* **73** 036131
- [22] Bonachela J A and Muñoz M A, *Phys. Rev. E* **78** 041102
- [23] Basu M, Basu U, Bondyopadhyay S, Mohanty P K and Hinrichsen H, 2012 *Phys. Rev. Lett.* **109** 015702
- [24] Dickman R, Tomé T and de Oliveira M J, 2002 *Phys. Rev. E* **66** 16111
- [25] Dhar D and Pradhan P, 2004 *J. Stat. Mech.: Theor. Exp.* **P0502**
- [26] Pradhan P and Dhar D, 2006 *Phys. Rev. E* **73** 021303
- [27] da Cunha S D, Vidigal R R, da Silva L R and Dickman R, 2009 *Eur. Phys. J. B* **72** 441
- [28] Dickman R, Alava M, Muñoz M A, Peltola J, Vespignani A and Zapperi S, 2001 *Phys. Rev. E* **64** 056104
- [29] Manna S S, 1990 *J. Stat. Phys.* **59** 509
- [30] Manna S S, 1991 *J. Phys. A: Math. Gen.* **24** L363
- [31] *GSL - GNU Science Library for C++*, URL: <http://www.gnu.org/software/gsl/>
- [32] de Oliveira M M and Dickman R, 2005 *Phys. Rev. E* **71** 016129
- [33] Dickman R and Kamphorst Leal da Silva J, 1998 *Phys. Rev. E* **58** 4266
- [34] Dickman R and de Oliveira M M, 2005 *Physica A* **357** 134